

## Deep and Bottom Water of the Weddell Sea's Western Rim

Arnold L. Gordon, Bruce A. Huber, Hartmut H. Hellmer,  
Amy Ffield

Oceanographic observations from the Ice Station Weddell 1 show that the western rim of the Weddell Gyre contributes to Weddell Sea Bottom Water. A thin (<300 meters), highly oxygenated benthic layer is composed of a low-salinity type of bottom water overlying a high-salinity component. This complex layering disappears near 66°S because of vertical mixing and further inflow from the continental margin. The bottom water flowing out of the western rim is a blend of the two types. Additionally, the data show that a narrow band of warmer Weddell Deep Water hugged the continental margin as it flowed into the western rim, providing the continental margin with the salt required for bottom-water production.

The South Atlantic's Weddell Gyre is the largest cyclonic gyre poleward of the Antarctic Circumpolar Current (1, 2), covering with its western part the Weddell Sea. Vigorous vertical fluxes of heat and moisture in the presence of a variable sea-ice cover couple Weddell waters with the cold polar atmosphere, making the Weddell Gyre a prime source of Antarctic Bottom Water (AABW). Sea ice covers nearly the entire Weddell Gyre in winter, retreating close to the Antarctic continent in summer, except in the western Weddell. Winter expeditions have examined the conditions in the central and eastern portions of the gyre (3), but its western rim, between 65° and 70°S and west of 50°W, had not been explored with modern field methods because of the difficulties of navigating the thick perennial ice cover there.

An effective way to gather extensive observations in the ice-cluttered western Weddell is to borrow a successful method from the Arctic: a scientific station on a drifting ice floe. The United States-Russian Ice Station Weddell 1 (ISW) was deployed on 11 February 1992 at 71°48'S and 51°43'W from the ice-breaking research vessel Akademik Fedorov. After a northward drift of 3.5 months and almost 700 km, the station and its occupants were recovered by Akademik Fedorov and RVIB Nathaniel B. Palmer on 9 June 1992 at 65°38'S and 52°25'W (Fig. 1). The drift of ISW followed closely the track of HMS Endurance, which was beset in the Weddell Sea ice on 18 January 1915 and sank on 21 November 1915 at 68°38'S and 52°26'W (4).

Oceanographic data obtained during the operation of ISW included 137 conductivity-temperature-depth (CTD) profiles from the ships during ISW deployment, recovery, and personnel-rotation cruises; at the ice camp along the drift track; and from

helicopters deployed along sections approximately normal to the drift track (hCTDs). Water samples were drawn at most of the sites for immediate analysis of salinity and dissolved-oxygen concentration. Additional samples were drawn for later analysis of H<sub>2</sub>, He, <sup>18</sup>O, and chlorofluorocarbons.

The thermohaline stratification in the western Weddell has the basic character of

the interior Weddell Gyre: a cold, low-salinity, surface-mixed layer separated by a rather weak pycnocline from a thick layer of relatively warm, salty deep water referred to as Weddell Deep Water (WDW) (Fig. 2). The WDW is characterized by core layers in which the temperature and salinity profiles exhibit maxima ( $T_{\max}$  and  $S_{\max}$  layers). Below this typical stratification, the ISW profiles display a thin, cold, oxygenated benthic layer (Fig. 2). In the region of the western Weddell sampled during ISW, the temperature-salinity (T-S) relation from the WDW  $T_{\max}$  to about 0°C is linear with little change between stations (Fig. 3). This section of the T-S relation represents the bulk of the water column below the WDW and is characteristic of the entire Weddell Gyre. The WDW  $T_{\max}$  and  $S_{\max}$  core water is drawn from the Circumpolar Deep Water into the Weddell Gyre at its eastern margin near 30°E (2, 5, 6), providing heat and salt to balance ocean and atmosphere exchanges within the Weddell Gyre. The lower, colder section of the nearly linear T-S curve represents the mixing of WDW with AABW which has been spatially and tem-

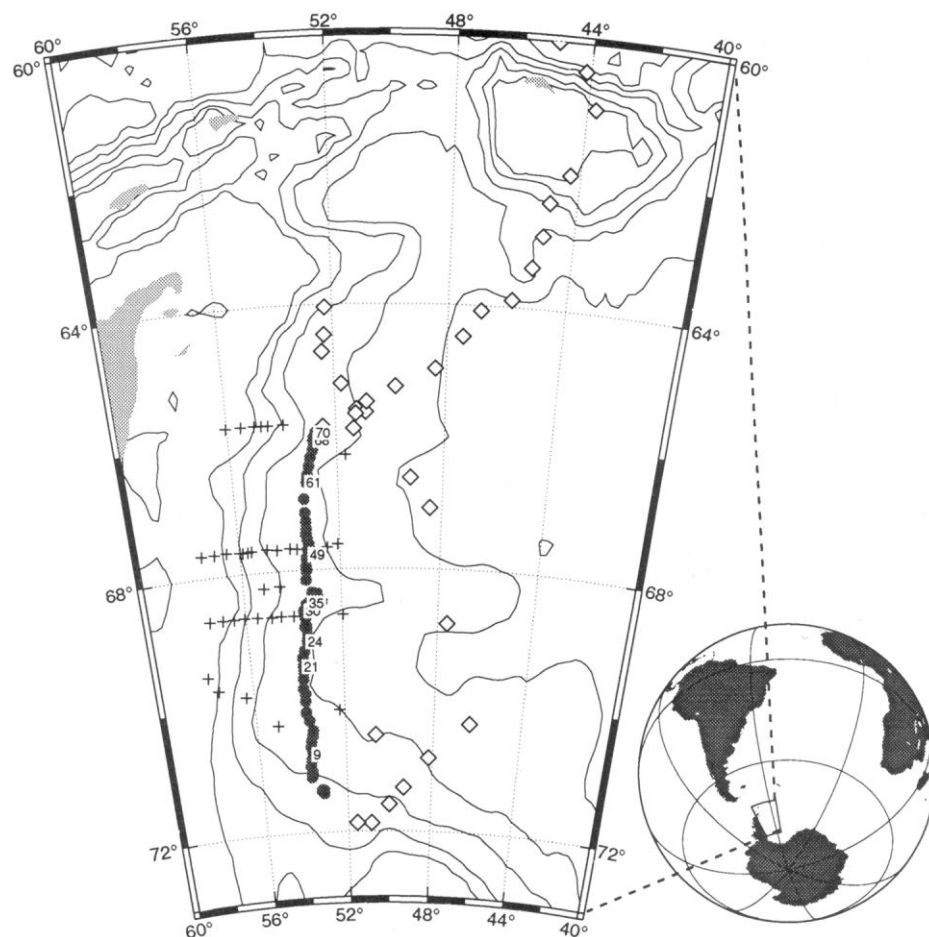


**Fig. 1.** Station map showing CTD profile locations from ships (diamonds), helicopters (+), and the ice station (shaded circles). Numbers identify ice-station CTD profiles whose data are shown in Figs. 2 and 3. Because existing bathymetric charts are unavailable for the ISW area, isobaths at 500, 1000, 2000, 3000, and 4000 m were constructed from recent aero-gravity and magnetics survey data (21).

porally homogenized over the gyre region.

The primary structure revealed in the ISW data that sets the western Weddell apart from the rest of the gyre is the thin benthic layer, which, by virtue of its cold temperature ( $< -0.8^{\circ}\text{C}$ ), may be referred to as Weddell Sea Bottom Water (WSBW) (7). The benthic layer is manifested in the T-S relation as a concavity below the linear portion, beginning at about  $-0.4^{\circ}\text{C}$  (Fig. 3). Although this part of the T-S curve is a visually dominant feature, it represents a boundary layer only about 200 m thick (Fig. 2). Minimum salinities in the benthic layers observed during ISW [about 34.60 practical salinity units (psu)] were lower than those reported for layers observed previously in the southwestern corner of the gyre (6). North of  $69^{\circ}40'\text{S}$  (Fig. 1, CTD 19), the low-salinity benthic layer is often underlain by a higher salinity bottom-water type ( $S > 34.62$  psu), which produces a local salinity minimum only 30 m above the sea floor. The low-salinity bottom-water type seems to bear a greater concentration of glacial melt (8). Along the ISW track to  $66^{\circ}26'\text{S}$ , the high-salinity type is present in varying amounts that show no correlation with bottom depth. The T-S structure indicates an origin from the salty shelf water of the southwestern Weddell (9), part of which has been observed at the southernmost hCTD (Fig. 3A), but hCTD data from farther north also indicate that salty contributions from that shelf are likely as well.

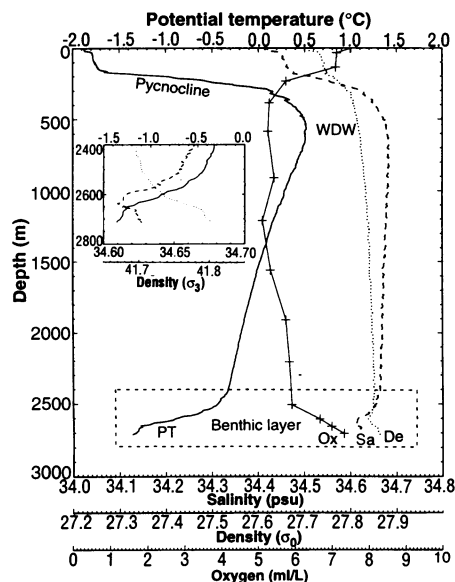


**Fig. 2.** Data from CTD profile 35. Includes potential temperature (PT), salinity (Sa), density (De) (referenced to density at surface), and oxygen concentration (Ox). This profile is typical of the ISW profiles along the continental slope. The depth of WDW is marked. (Inset) Enlargement of benthic layer. It shows stable stratification with potential density referenced to 3000 m ( $\sigma_3$ ).

The benthic-layer water can be traced to slope plumes forced by export of various shelf-water types, with a likely role for cabbeling and thermobaric processes (9–11). A mixing line drawn from the base of the linear part of the T-S curve through the low-salinity WSBW end-member passes through T-S points of near-bottom shelf water (Fig. 3B). The cold shelf water becomes unstable to convection as pressure is exerted by downwelling over the continental slope. Downwelling may be initiated by Ekman veering and cabbeling, with thermobaric effects providing the positive feedback that allows slope plumes to reach the bottom (9, 10).

The top of the benthic layer is marked by a weak pycnocline, which amounts to a

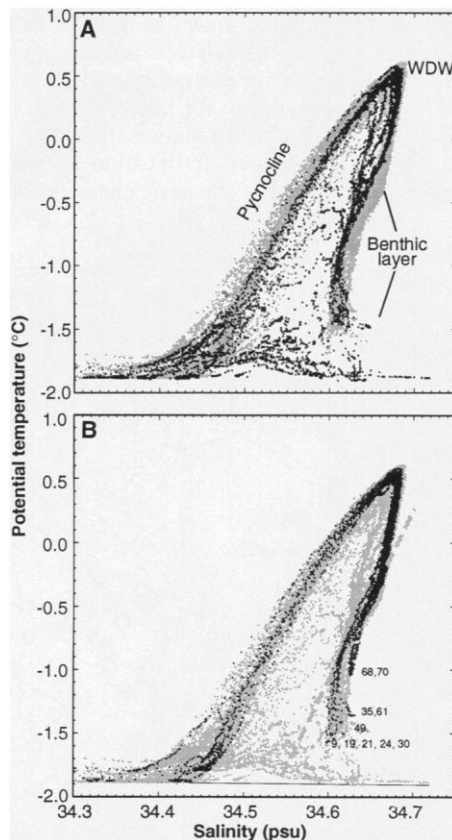


**Fig. 3.** Composite T-S relation. (A) hCTD data for stations west of the drift track. (B) Ice-station data from locations along the track chosen to exemplify development of the benthic boundary layer; the station numbers match those in Fig. 1. The data are superimposed on the envelope of all ISW data (shaded). The WDW core is marked at a  $T_{\max}$  and  $S_{\max}$  near  $0.5^{\circ}\text{C}$  and 34.68 psu found near 500 m, below which the T-S curve is nearly a straight line. For deep water colder than about  $-0.4^{\circ}\text{C}$ , the curve is concave, depicting the thin benthic layer. The dashed line (shaded) in (B) is a possible mixing curve indicating near-bottom shelf water as a possible source for the low-salinity WSBW type. The thin, solid line in (B) represents the freezing point for surface waters.

density gradient of only  $0.1 \text{ kg m}^{-3}$  over 300 m. Near  $66^{\circ}\text{S}$ , the thin benthic layer abruptly thickens to as much as 800 m. In the T-S relation, the bottom part of the curve moved toward warmer saltier water to occupy the T-S cavity formed by the double water-type arc (Fig. 3B, stations 68 and 70), whereas the portion of the curve between  $-0.6^{\circ}\text{C}$  and  $0.1^{\circ}\text{C}$  moved toward lower salinity. The mean potential temperature and salinity of the water column deeper than the  $0.2^{\circ}\text{C}$  isotherm north of  $66^{\circ}\text{S}$  is colder and fresher than that to the south (12). Thus, the increase in benthic-layer thickness is the result of further contribution of low-salinity WSBW from the western edge of the Weddell, rather than a simple (one-dimensional) mixing phenomena. What finally emerges from the western Weddell is AABW of the type observed in archived data (13). It gives little hint of the complex layering and multiple water types involved in the origin of this globally important water mass.

The contribution from the shelf to newly formed bottom water colder than  $-0.8^{\circ}\text{C}$  (14) is estimated to be less than  $3 \times 10^6 \text{ m}^3 \text{ s}^{-1}$ . This estimate was derived with the assumption of a spatially continuous down-slope flow that crosses the ISW track at an unknown angle in a layer whose thickness is the average thickness of the benthic layer observed in the ISW data. Because direct

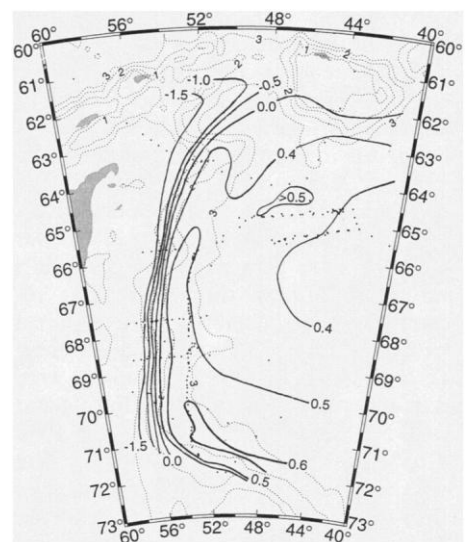


**Fig. 4.** Temperature (in degrees Celsius) at the core of the WDW ( $T_{\max}$ ). The narrow band of  $T_{\max}$  water warmer than  $0.5^{\circ}\text{C}$  overlying the continental slope (depths between 2000 and 3000 m) may be a continuous feature from the Greenwich Meridian, advected into the western Weddell by the outer-limb or rim-current component of the western boundary current. Heavy dots represent a combination of ISW stations and historical stations from 1986 to 1989. Contours of depth in thousands of meters are marked by light dotted lines.

measurements of bottom-current speed are unavailable in the ISW region, a flow speed of  $7 \text{ cm s}^{-1}$  was assumed, on the basis of measurements of outflow from the Filchner Depression, to the southeast of the ISW region (15). To account for the observed increase in the thickness of the benthic layer, we used average thickness values of 70 and 240 m for the regions south and north of  $66^\circ\text{S}$ , respectively. As a consequence of this subdivision, 30% of the estimated shelf-water contribution originates from the area north of  $66^\circ\text{S}$ .

Data collected from the upper water column during ISW reveal that a narrow band of  $T_{\text{max}}$  water  $>0.5^\circ\text{C}$  flowed along the western edge of the Weddell Sea over the continental slope (Fig. 4). This feature may extend from its first appearance near the Greenwich Meridian (16) covering a distance of 2000 km. Cooling of the  $T_{\text{max}}$  layer en route from near  $1.0^\circ\text{C}$  at the Greenwich Meridian to  $0.5^\circ\text{C}$  at the northern end of the ISW data array represents attenuation by vertical and isopycnal processes that expose the WDW core to cold surface and continental-shelf water masses. In the western Weddell, a more stable layer within the pycnocline is observed in the 200- to 300-m interval, with the WDW  $T_{\text{max}}$  at 500 to 600 m. This stands in sharp contrast to the shallow (at the base of the winter mixed layer near 110 m) pycnocline and the warmer  $T_{\text{max}}$  ( $>0.8^\circ\text{C}$  within the 150- to 250-m interval) of the eastern section of the Weddell Gyre (3). This stratification difference may account for different vertical heat fluxes observed in the two regimes (3, 17) and associated perennial ice cover of the western Weddell.

With the Weddell Gyre's center well east of the ISW survey, generally between  $20^\circ$  and  $40^\circ\text{W}$  (2), the baroclinic expression of the western boundary current appears to be over 400 km wide. However, the distribution of the  $T_{\text{max}}$  along the western rim of the Weddell Gyre distinguishes two components of the western boundary current: A rim current that advects the warmest water from the eastern margins of the gyre to the western edge and a longer residence interior component, basically a recirculation of the inner hub of the gyre (16, 18). The rim current is likely to be more important to the overall water-mass formation processes, as it provides the salt required for bottom-water formation to the continental margins. Determination of geostrophic shear with the thermal wind equation, with adjustment to the order of the current speed observed in the near-surface layer at ISW (19), indicates that the rim-current transport is about  $10 \times 10^6$  to  $15 \times 10^6 \text{ m}^3 \text{ s}^{-1}$ . The interior recirculation flow is unknown, but it may be larger than  $10 \times 10^6 \text{ m}^3 \text{ s}^{-1}$  with a mean bottom-current

speed of  $1.3 \text{ cm s}^{-1}$  as a reference, as measured at  $66^\circ30'\text{S}$  and  $41^\circ\text{W}$  (20), transport of over  $30 \times 10^6 \text{ m}^3 \text{ s}^{-1}$  is likely, producing a total western boundary transport of about  $40 \times 10^6 \text{ m}^3 \text{ s}^{-1}$ .

## REFERENCES AND NOTES

1. G. E. R. Deacon, *Deep-Sea Res.* 26, 981 (1979).
2. A. Orsi, W. Nowlin, T. Whitworth, *ibid.* 40, 169 (1993).
3. A. Gordon and B. Huber, *J. Geophys. Res.* 95, 11655 (1990).
4. E. Shackleton, *South* (MacMillan, New York, 1920).
5. N. Bagriantsev, A. Gordon, B. Huber, *J. Geophys. Res.* 94, 8331 (1989).
6. V. V. Gouretski and A. I. Danilov, *Deep-Sea Res.* 40, 561 (1993).
7. T. Foster and E. Carmack, *ibid.* 23, 301 (1976).
8. P. Schlosser, personal communication.
9. A. Foldvik, T. Gammelsrød, T. Tørresen, *Antarct. Res. Ser.* 43, 5 (1985).
10. A. Gill, *Deep-Sea Res.* 20, 111 (1973).
11. Cabbelling refers to the mixing of two parcels of seawater with different temperature and salinity but similar densities. Because of the nonlinear equation of state for seawater, such mixtures can produce a parcel that is denser than the two constituent parcels. Thermobaricity is a property of seawater at temperatures below which the compressibility of seawater is significant in the determination of its density. As a parcel of water at sufficiently low temperature is subject to in-
12. This isotherm falls well within the linear  $T$ - $S$  segment and hence is above the influence of the local benthic layer. The average potential temperature of the deep and bottom water below the  $0.2^\circ\text{C}$  isotherm decreases by  $0.25^\circ\text{C}$  from station 64 to station 70, coinciding with a thickening of the benthic layer. The corresponding salinity is reduced by 0.015 psu. This suggests additional injection of WSBW into the benthic layer north of  $66^\circ\text{S}$ .
13. E. Carmack, in *A Voyage of Discovery* (Pergamon, New York, 1977), pp. 15–42.
14. ———, *Deep-Sea Res.* 21, 431 (1974).
15. A. Foldvik, T. Kvinge, T. Tørresen, *Antarct. Res. Ser.* 43, 21 (1985).
16. T. Whitworth and W. Nowlin, *J. Geophys. Res.* 92, 6462 (1987).
17. M. McPhee, J. Morison, D. Martinson, *Eos* 73, 308 (1992).
18. A. Gordon, in *Antarctic Ocean and Resources Variability* (Springer-Verlag, Berlin, 1988).
19. R. Muench, J. Gunn, M. Morehead, *Eos* 73, 301 (1992).
20. T. Foster and J. Middleton, *Deep-Sea Res.* 26, 743 (1979).
21. J. Labrecque and M. Ghidella, *J. Geophys. Res.*, in press.
22. Funded by NSF grant DPP 90-24577. We thank J. Ardai, R. Guerrero, G. Mathieu, S. O'Hara, and R. Weppernig for help collecting the CTD data, and W. Haines and P. Mele for data processing. This is contribution 5101 of Lamont-Doherty Earth Observatory.

28 April 1993; accepted 15 July 1993

## Pressure-Induced Enhancement of $T_c$ Above 150 K in Hg-1223

M. Nuñez-Regueiro,\* J.-L. Tholence, E. V. Antipov, J.-J. Capponi, M. Marezio†

The recently discovered homologous series  $\text{HgBa}_2\text{Ca}_{n-1}\text{Cu}_n\text{O}_{2n+2+\delta}$  possesses remarkable properties. A superconducting transition temperature,  $T_c$ , as high as 133 kelvin has been measured in a multiphase Hg-Ba-Ca-Cu-O sample and found to be attributable to the Hg-1223 compound. Temperature-dependent electrical resistivity measurements under pressure on a ( $>95\%$ ) pure Hg-1223 phase are reported. These data show that  $T_c$  increases steadily with pressure at a rate of about 1 kelvin per gigapascal up to 15 gigapascals, then more slowly and reaches a  $T_c = 150$  kelvin, with the onset of the transition at 157 kelvin, for 23.5 gigapascals. This large pressure variation (as compared to the small effects observed in similar compounds with the optimal  $T_c$ ) strongly suggests that higher critical temperatures could be obtained at atmospheric pressure.

In analogy with the Bi- and Tl-based superconducting copper oxides, the structures of the  $\text{HgBa}_2\text{Ca}_{n-1}\text{Cu}_n\text{O}_{2n+2+\delta}$  series are constructed with  $n \text{ CuO}_2$  layers sandwiched between rock-salt  $(\text{BaO})(\text{HgO})_2(\text{BaO})$

blocks. In comparison with the former, the Hg compounds yield noticeably higher conducting/superconducting transition temperatures, namely 94, 129, 133, and 126 K for the  $n = 1, 2, 3$ , and 4 compounds, respectively (1–3). The synthesis of the compounds is complicated by the low decomposition temperature of HgO. High pressure hinders this decomposition and facilitates the formation reactions. However, it is still not clear if the measured values of  $T_c$  are optimal. Besides the empirical method of changing the preparation conditions and stoichiometry, there is another way of checking this. It is now generally accepted (4–6) that application of high pressures up

M. Nuñez-Regueiro and J.-L. Tholence, Centre de Recherches sur les Très Basses Températures, CNRS-UJF, BP 166 Cedex 9, 38042 Grenoble, France. E. V. Antipov, Department of Chemistry, Moscow State University, 119899 Moscow, Russia. J.-J. Capponi and M. Marezio, Laboratoire de Cristallographie, CNRS-UJF, BP 166 Cedex 9, 38042 Grenoble, France.

\*On leave of absence from Centro Atómico Bariloche, 8400 Bariloche, Argentina.

†Also at AT&T Bell Laboratories, Murray Hill, NJ 07974.